



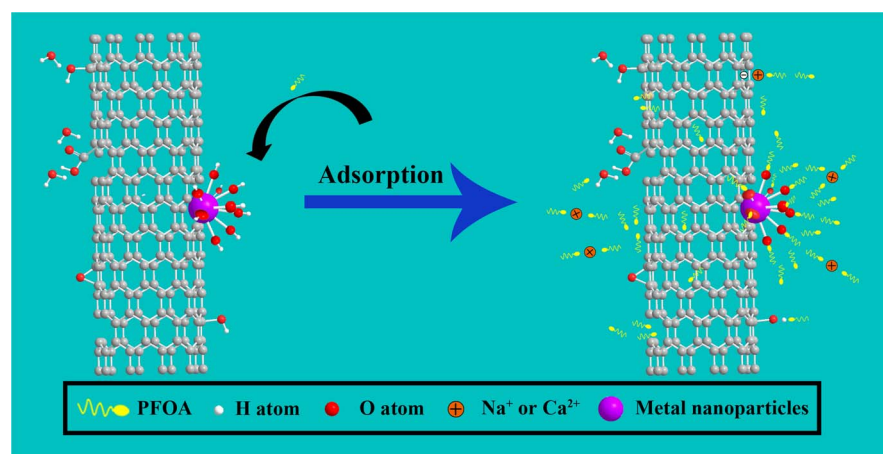
Metal nanoparticles by doping carbon nanotubes improved the sorption of perfluorooctanoic acid

Longfei Liu^a, Deyun Li^a, Chengliang Li^{a,*}, Rong Ji^{b,*}, Xiaofei Tian^a

^a National Engineering Laboratory for Efficient Utilization of Soil and Fertilizer Resources, College of Resources and Environment, Shandong Agricultural University, Tai'an, 271018, China

^b State Key Laboratory of Pollution Control and Resource Reuse, School of the Environment, Nanjing University, Nanjing, 210046, China

GRAPHICAL ABSTRACT



ARTICLE INFO

Keywords:

Metal nanoparticles
Grafted
Carbon nanotubes
Adsorption
PFOA

ABSTRACT

Due to considerable application of perfluorooctanoic acid (PFOA) and its refractory degradation, the widespread distribution of PFOA has already resulted in its risks to environment and organisms. However, the intrinsic characteristic of pristine multi-walled carbon nanotubes (MWCNTs) limited their application for removing PFOA from aqueous medium. Therefore, three nano-metals (nano-crystalline iron, copper and zinc) grafted MWCNTs were synthesized and characterized by BET-N₂, TEM, FTIR, XPS and XRD as well as MWCNTs (as the control treatment) in this study. The results showed that nano metals were well grafted on the surface of MWCNTs. Adsorption were investigated by using radioactive labeled PFOA (¹⁴C-PFOA) to quantify the trace PFOA. Adsorption kinetics showed the adsorption of PFOA on the metal doped MWCNTs (MDCNTs) was controlled by intra-particle diffusion. Adsorption isotherms showed the sorption amounts on the MDCNTs were higher than the control. This attributed much to the hydrophobic interaction, electrostatic interaction and the formation of the inner sphere complexes. Ionic strength (0–100 mM) and ionic species (Ca²⁺) had little effects on the sorption of MDCNTs. PFOA adsorption on MDCNTs strongly depended on pH value in the medium. These results provide an innovative approach for removing trace PFOA from liquid medium.

* Corresponding authors.

E-mail addresses: chengliang_li11@163.com (C. Li), ji@nju.edu.cn (R. Ji).

<https://doi.org/10.1016/j.jhazmat.2018.03.001>

Received 24 September 2017; Received in revised form 6 February 2018; Accepted 1 March 2018

Available online 08 March 2018

0304-3894/ © 2018 Elsevier B.V. All rights reserved.

1. Introduction

Perfluorooctanoic acid (PFOA) is widely used in many products in the past more than half a century because of its high surface activity, resistance to acid and alkali and unique thermal stability [1–4]. Due to the large-scale application of PFOA and its precursors, considerable PFOA was released to the environment [5–7]. The high stability of PFOA is mainly due to the huge energy of C–F covalent bond ($531.5 \text{ kJ mol}^{-1}$) [8]. Therefore, considerable PFOA existed in the surface water, soil, atmosphere, sediment and biota for a long time, and PFOA significantly possessed biological accumulation and amplificative characteristics [1,2,9–12]. Some researchers concluded that water was one of the most important backgrounds for PFOA entering human body [13], and PFOA showed a series of toxic effects [14,15]. PFOA had a half-life of about 3.8 years in the human body [16], and the detriment to human is persistent, so it is urgent to remove PFOA from water, especially in drinking water.

Nevertheless, because of the chemically inert and high thermal stability, PFOA molecules are difficult degraded by natural processes [17,18]. As reported, there are several common methods for PFOA degradation [19–21]. However, some of these methods are very expensive or require vast amounts of energy in the degradation processes. In addition, some of these methods use hydroxyl radicals to scavenge PFOA, which was reported that the removal efficiency was not good [22].

Adsorption method for removing perfluorinated compounds is comprehensively accepted as an effective, low energy consumption and environment friendly method [23,24]. Some common adsorbents, such as activated carbon, had been used to adsorb perfluorochemicals in aqueous solution [25–30]. But the adsorption capacities were not optimistic. Some studies found that biological activated carbon was not effective enough for removing trace PFOA in drinking water [31]. In addition, there was an experiment to prove that after using one kind of conventional coagulants ($\text{FeCl}_3 \cdot 6\text{H}_2\text{O}$) for adsorbing PFOA, the removal ratio of PFOA was only about 12% [32]. Hence, new adsorbents with high adsorption capacity, good recyclability, and low cost are urgently needed to be invented or ameliorated.

Carbon nanotubes have attracted more and more attention due to their unique one-dimensional hollow tubular structure, large specific surface area, and strong adsorption capacity [33]. The adsorption of multi-walled carbon nanotubes (MWCNTs) on some pollutants showed excellent results than traditional adsorbents [34]. However, after being treated by strong acid to remove the independent amorphous carbons and residual catalysts, the surface of MWCNTs were loaded by hydrophilic functional groups (e.g. hydroxyl and/or carboxyl). This would encourage MWCNTs to combine with water molecules or to weaken the hydrophobic interaction, and consequently inhibit the adsorption amount of PFOA [35].

In the last several years, most researches of nano-complexes focused on the fields such as catalyst, super capacitor and super battery [36–38]. Some researchers reported that the residual of metal catalyst particles remaining on MWCNTs can promote the adsorption of PFOA on MWCNTs [24]. Nowadays, there is no literature on the adsorption of PFOA in aqueous solution by metal doped MWCNTs. Therefore, a conjecture was proposed that compared with the MWCNTs and commonly used treatment (strong acid or strong oxidant treatment) of MWCNTs, metal doped MWCNTs may improve the adsorption capacity of PFOA.

In this study, different metal nanoparticles were grafted on the surface of MWCNTs by various approaches, and the metal doped MWCNTs were characterized. The adsorption mechanism(s) of PFOA on them was determined by batch technique. Simultaneously, the effects of ionic strengths, ionic species, and electrolyte pH values on the adsorption of PFOA were also investigated. It is hoped that the data and results of this study are helpful for understanding the adsorption behavior of PFOA on metal doped MWCNTs in water environment.

2. Materials and methods

2.1. Chemicals

Non-labeled PFOA (96% purity) and ^{14}C -labeled PFOA (99% radiochemical purity and 55 mCi mmol^{-1} specific activity) were purchased from KMF Laborchemie Handels GmbH (Germany) and American Rediolabeled Chemicals, Inc. (USA), respectively. The selected physical-chemical properties of PFOA are listed in Table S1. Stock solutions were prepared by mixing non-labeled and ^{14}C -labeled PFOA in Milli-Q water and stored at 4°C . MWCNTs were purchased from Shenzhen Nanotech Port Co., China. Other chemical reagents for grafting metal nanoparticles (MNPs) are analytical reagent levels.

The grafted MWCNTs were synthesized according to available literatures [39,40]. Nano zinc loading method was referenced to loaded nano iron, and then marked as $\text{Fe}/\text{Fe}_2\text{O}_3\text{-CNTs}$, $\text{Cu}/\text{CuO-CNTs}$ and $\text{Zn}/\text{ZnO-CNTs}$ ($\text{X}/\text{XO}_y\text{-CNTs}$, $\text{X} = \text{Fe}, \text{Cu}, \text{Zn}$ and $y = 1$ or $3/2$), respectively.

In order to avoid the adsorption of PFOA by the independent MNPs, all of the complexes were washed repeatedly with ultrasonic treated 95% ethanol by suction filtration ($0.45 \mu\text{m}$ filter membrane), to remove the MNPs that did not firmly load on the surface of the MWCNT.

2.2. Characterization of $\text{X}/\text{XO}_y\text{-CNTs}$ and MWCNTs

The zeta potentials of $\text{X}/\text{XO}_y\text{-CNTs}$ and MWCNTs were probed by the zeta potentials-pH curves using a laser particle size analyzer (Zetasizer Nano S, UK). The specific surface area (SSA) of adsorbents were determined by nitrogen adsorption-desorption isotherms at 77 K that were measured using NOVA 4000e (Quantachrome, USA) through multipoint Brunauer-Emmett-Teller (BET) method. Microscopy images were observed by field emission transmission electron microscopy (FETEM, Tecnai G2 F20, USA) and the crystalline interplanar spacing were demarcated and measured by Gatan DigitalMicrograph 3.9. Powder X-ray diffraction (XRD, Bruker D8 Venture, Germany) with $\text{Cu K}\alpha$ radiation was used to identify the phase composition and crystal lattice parameters of textured samples and the patterns were analyzed by MDI Jade 5.0 software. The diffraction patterns were collected at room temperature by step scanning in the range of $15^\circ\text{--}85^\circ$ at a scanning rate of $12^\circ \text{ min}^{-1}$. The surface functional groups were observed by X-ray photoelectron spectroscopy (XPS, Thermo Escalab 250Xi, USA) and Fourier transform infrared spectroscopy (FTIR, Thermo Fisher, USA). The XPS data were collected with an energy step size of 1.00 eV and the spectra were analyzed by Thermo Advantage software. The FTIR spectras were recorded on the spectrum in the $4000\text{--}400 \text{ cm}^{-1}$ region with a resolution of 2 cm^{-1} in transmission mode.

2.3. Adsorption and desorption experiments

Adsorption kinetics and isotherms were investigated by using batch equilibration technique and all the experiments were performed in three replications. Some studies found that equilibration time had no effect on initial environmental factors [41]. Therefore $500 \mu\text{g L}^{-1}$ of PFOA as the initial concentration was to determine adsorption kinetics. The adsorbents (1.2 mg) were weighted into polypropylene tubes, and pre-wetted with 10 mmol L^{-1} NaCl and 200 mg L^{-1} NaN_3 (to prevent biodegradation) electrolyte solution (12 mL) for 24 h . The electrolyte solution had been adjusted to $\text{pH } 6.50 \pm 0.10$ using 0.1 mol L^{-1} HCl or NaOH . Then aliquot of ^{14}C - and non-labeled PFOA stock solution ($20 \mu\text{L}$) was added into tubes. All tubes were mixed at 150 rpm on a horizontal shaker at $25 \pm 1^\circ\text{C}$ and the whole process was carried out under shading conditions. The solid and liquid phases were separated by centrifugation for 20 min at $10,000g$ [24]. The radioactivity in the supernatant was detected using liquid scintillation counter.

For adsorption isotherms, adsorbents were weighted into polypropylene tubes respectively and pre-wetted with electrolyte solution as

the same as adsorption kinetics. Aliquot volumes of PFOA stock solution (20 μL) were added into the tubes to reach PFOA concentrations range (18 $\mu\text{g L}^{-1}$ –500 $\mu\text{g L}^{-1}$). All tubes were homogeneously mixed on a horizontal shaker (150 rpm) for 24 h, which was obtained based on the adsorption kinetic. The whole process was also carried out under shading conditions. The supernatant were obtained for radioactive determination after centrifuging for 20 min at 10,000g.

Desorption experiments were carried out immediately after adsorption equilibrium (Fig. S1). A half volume of the supernatant was taken out, and the same volume of PFOA-free electrolyte solution was added. Then all tubes were homogeneously mixed on horizontal shaker (150 rpm) for 24 h. The operation of desorption experiments were carried out six times as the same as the above process.

The influences of ionic strength and pH on PFOA adsorption were investigated with an initial concentration of 200 $\mu\text{g L}^{-1}$ PFOA. For the ionic strength experiments, adsorption processes were implemented in 0–100 mmol L^{-1} NaCl solutions (pH 6.50 ± 0.10). NaCl and CaCl_2 were chosen as ionic species and controlling the same ionic strength as 10 mmol L^{-1} . The pH experiments were carried out in pH 4–10 using 10 mmol L^{-1} NaCl as electrolyte solution.

2.4. Radioactive determination

1.00 mL supernatant was mixed with 4.00 mL scintillation cocktail (Gold Star multipurpose, Meridian Biotechnologies Ltd., UK) in dedicated vial and then counted on a liquid scintillation counter (LSC, Beckman Coulter LS-6500, USA) for 5 min [24].

2.5. Data analysis

Four adsorption kinetic models, i.e. pseudo-first-order model, pseudo-second-order model, intra-particle diffusion model and Boyd model were used to describe the adsorption rates and equilibrium times. Two models, Henry and Freundlich, were employed to simulate sorption isotherms. The details of these models were expressed in Part II A of Supplementary data. In addition, all the functional graphs were produced using Origin 8.6 software (OriginLab, USA).

3. Results and discussion

3.1. Characterization of adsorbents

3.1.1. Basic physic-chemical information of X/XO_y-CNTs and MWCNTs

Metal nanoparticles were grafted on the surface of MWCNTs via the reduction method. Their characteristics were listed in Table 1. Compared to the MWCNTs, the SSA, pore volume and pore size of X/XO_y-CNTs were significantly lower. At the same time, the ash contents of X/XO_y-CNTs were significantly augmented after grafting. Elemental analytical results illustrated that the mass content of Fe, Cu and Zn and

their oxides on the MWCNTs surface were 8.46%, 7.73% and 9.73%, respectively. The concentrations of O and H elements of X/XO_y-CNTs were pronouncedly enhanced while the content of C element was markedly decreased in comparison with MWCNTs. In addition, the surface acid amounts of carboxyl and hydroxyl groups on the X/XO_y-CNTs were 1.11–1.63 mmol g^{-1} and 2.11–3.74 mmol g^{-1} in comparison with MWCNTs.

Zeta potentials of the four adsorbents used in the experiments are shown in Fig. S2. The zero points of Fe/Fe₂O₃-CNTs and Cu/CuO-CNTs were pH 6.1 and 7.2, respectively, and that of Zn/ZnO-CNTs and MWCNTs were less than pH 4. This suggested that Fe/Fe₂O₃-CNTs and Cu/CuO-CNTs were more easily protonated than Zn/ZnO-CNTs and MWCNTs.

3.1.2. XRD analysis

Crystal phases of the nano-composites were investigated by XRD analysis and the patterns were demonstrated in Fig. 1. The properties of the X/XO_y-CNTs were similar to those reported in the references (see the Part II B of Supplementary data). Interestingly, compared with MWCNTs (Fig. 1D), the X/XO_y-CNTs had distinct weak (002) diffraction peaks at about 26. What's more, the peaks of (101) of graphite disappeared in the doped ones. This phenomenon suggested that the incorporation of nano-metals altered or even destroyed a part of structures of MWCNTs, or served as an interval to separate graphene sheets of MWCNTs [44–46].

3.1.3. TEM analysis

The Fe, Cu and Zn nano-crystals and MWCNTs were clearly shown in HRTEM images (Fig. S8). The nano-metals distributed on the surface of MWCNTs with irregular spherical shape, and most of the nano-metals had a slightly agglomeration phenomenon, especially the nano-iron and nano-copper. Some nano-metals entered into the interlayers of MWCNTs, which were consistent with the XRD measurement (Fig. 1A–C) [44]. Therefore, there were many defects on the surface of the X/XO_y-CNTs, which led to more adsorption sites on the surface of it. The resulting defects on the surface were expected to be advantageous for the adsorption capacity of adsorbents [47].

3.2. Adsorption–desorption of PFOA by X/XO_y-CNTs and MWCNTs

3.2.1. Adsorption kinetics

PFOA adsorption kinetics onto adsorbents over time were illustrated in Fig. 2. In order to study the controlling mechanism(s), four different kinetic models were used to analyze the transient behavior, and the relevant parameters obtained through model fitting were presented in Table S2. According to the adjusted square correlation coefficients (r_{adj}^2), the pseudo-second-order model was more suitable to describe the adsorption behavior of PFOA on X/XO_y-CNTs and MWCNTs.

In Fig. 2A, the sorption rate of PFOA on adsorbents were very fast in

Table 1
Physic-chemical properties of X/XO_y-CNTs and MWCNTs.

Adsorbent	SSA _{BET} ($\text{m}^2 \text{g}^{-1}$)	MV _{DFT} ^a ($\text{cm}^3 \text{g}^{-1}$)	MW _{DFT} ^b (nm)	Ash ^c (%)	Amount of surface acid ^d (mmol g^{-1})			Elemental content ^e (%)					
					Carboxyl	Lactones	Hydroxyl	C	H	O	Fe	Cu	Zn
MWCNTs	114.10	$8.18 \cdot 10^{-2}$	2.95	1.86	– ^f	–	–	93.27	0.35	6.18	–	–	–
Fe/Fe ₂ O ₃ -CNTs	82.84	$3.15 \cdot 10^{-2}$	2.09	10.54	1.33	0.08	2.51	72.48	1.18	17.81	8.46	–	–
Cu/CuO-CNTs	92.53	$4.44 \cdot 10^{-2}$	2.32	10.08	1.63	0.07	2.11	75.88	1.13	15.13	–	7.73	–
Zn/ZnO-CNTs	77.29	$5.12 \cdot 10^{-2}$	2.65	11.70	1.11	0.10	3.74	69.46	1.82	19.35	–	–	9.73

^a Micropore volume.

^b Micropore width were calculated by density functional theory.

^c Ash content was measured by heating the adsorbents at 950 °C for 5 h.

^d Amount of surface acid were calculated by acid-alkali neutralization titration method [42].

^e C, H and O elements were measured by elemental analyzer and the nano-metal (Fe, Cu and Zn) content were determined by ICP-MS [43].

^f Content was not detected.

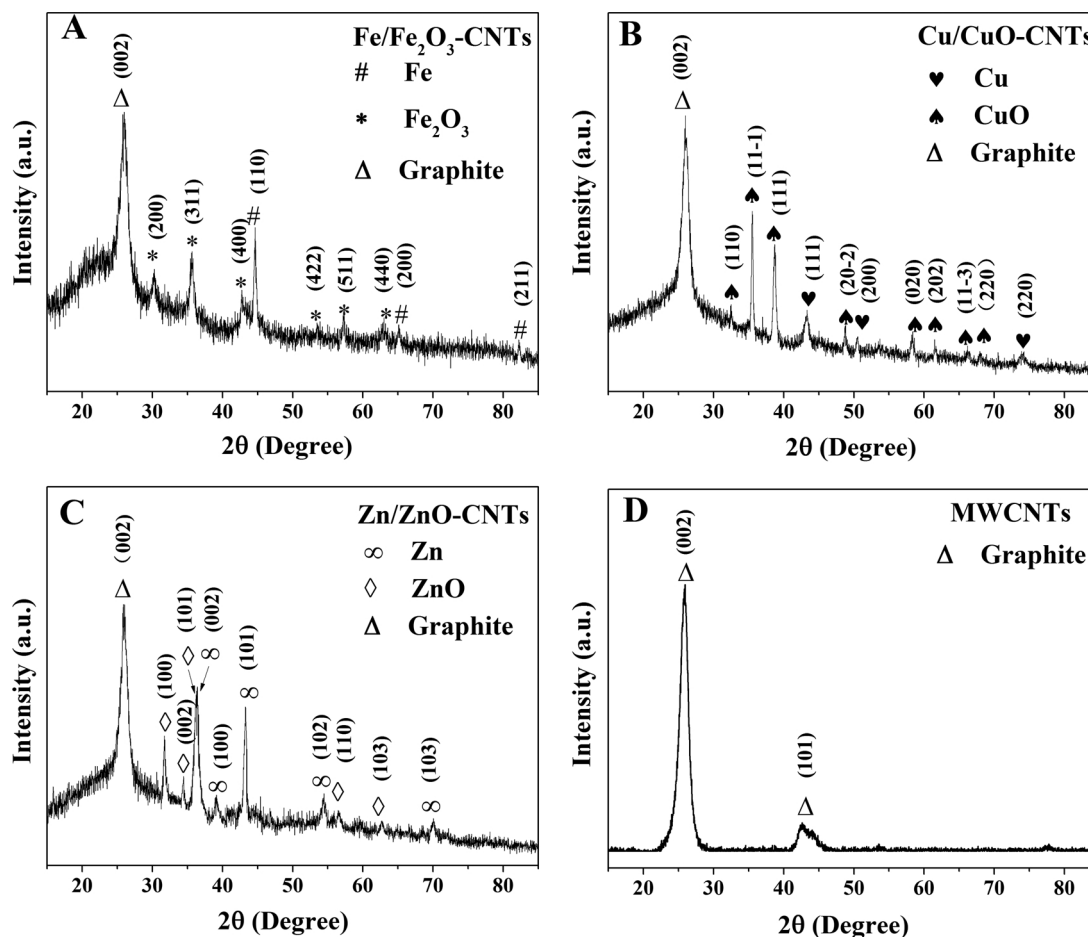


Fig. 1. XRD patterns of (A) Fe/Fe₂O₃-CNTs, (B) Cu/CuO-CNTs, (C) Zn/ZnO-CNTs and (D) MWCNTs.

the initial 60 min, and the adsorption equilibrium were reached after 12 h. This was because in the initial adsorption stage, adsorbents surface had a large number of adsorption sites, which can rapidly and substantially adsorb PFOA molecules. At the latter stage, due to the repulsion between PFOA molecules, the sorption rate decreased [48]. In Table S2, it can be intuitively understood that the initial sorption rate of X/XO_y-CNTs, v_o , were higher than that of the MWCNTs. This involved a rapid chemical reaction between carboxyl of PFOA and hydrous MNPs, while the sorption on MWCNTs had no this fast process [49].

As shown in Fig. 2B, there were two regions and the straight part did not pass the origin point. This indicated that the sorption was controlled by surface adsorption (curved portion, 0–17.32 min^{1/2}) and intra-particle diffusion (linear portion, 18.97–53.67 min^{1/2}) [49]. K_i values

were the calculated value of slope in the straight-line portion and the intercept of fitting line mirrored the boundary layer effect. As the intercept increase, the dedication of the surface sorption in the rate controlling step increased. Thus, the PFOA adsorption on X/XO_y-CNTs and MWCNTs was controlled by both surface adsorption and intra-particle diffusion.

For better analysis the controlling step, Boyd model was the procedure given to analyze kinetic data and the plot was demonstrated in Fig. 2C. Boyd equation reflected particle diffusion, which is the diffusion through or into the adsorbent. B_t is a single constant of Boyd equation and its value is ascertained by the ratio of the particle to the square of the particle radius, which is confirmed by the inter-particle diffusion constant. The fitting line passed through the origin point

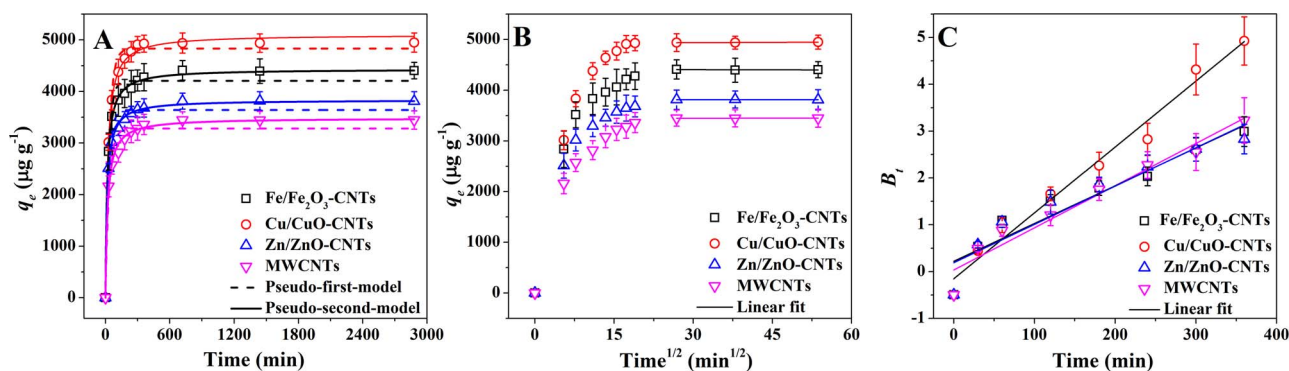


Fig. 2. (A) Pseudo-first-order model (the dashed line) and pseudo-second-order model (the solid line), (B) intra-particle diffusion model and (C) Boyd model of PFOA adsorption kinetics on four kinds of adsorbents.

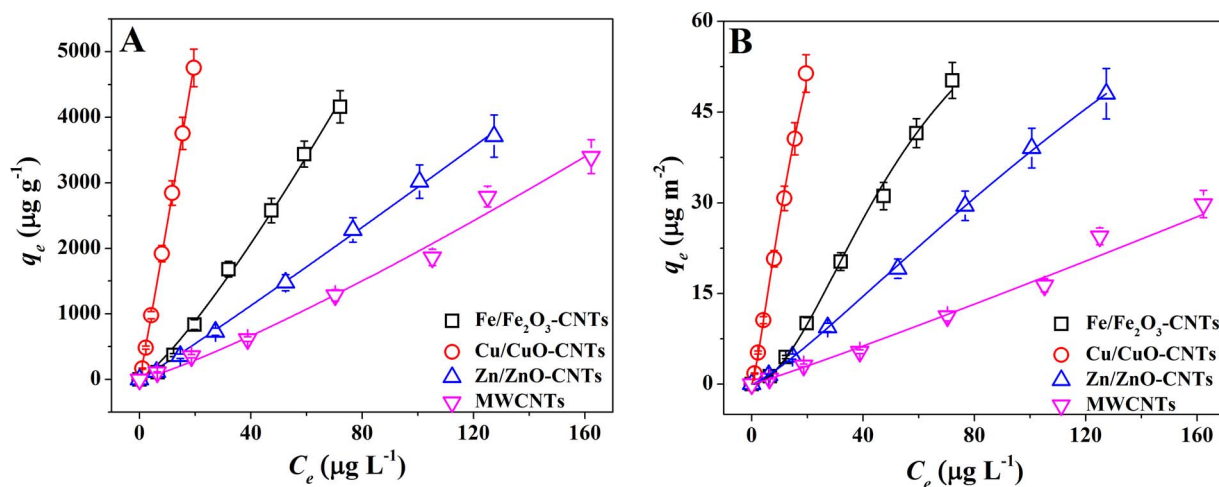


Fig. 3. Adsorption isotherms of PFOA onto X/XO_y-CNTs and MWCNTs. (A) Solid-phase concentrations were expressed by the unit of $\mu\text{g L}^{-1}$, and (B) solid-phase concentrations were expressed by the unit of $\mu\text{g m}^{-2}$. The solid lines represented isotherms fitted by Freundlich model.

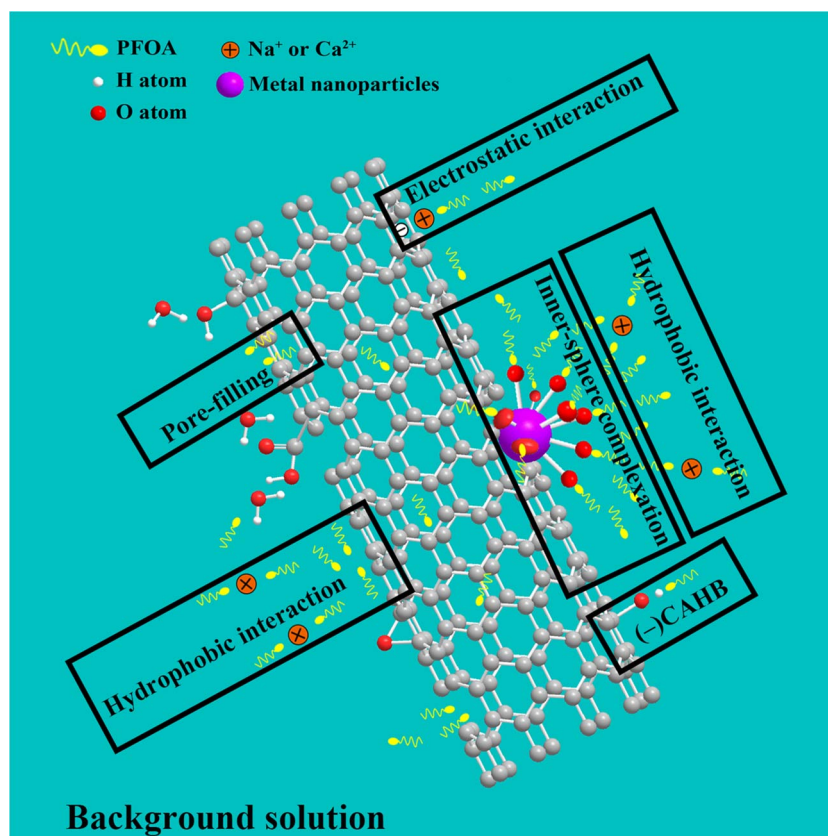


Fig. 4. The diagrammatic sketch of main mechanisms about PFOA adsorbed on X/XO_y-CNTs.

which confirmed intra-particle diffusion to be the rate controlling step [49].

3.2.2. Adsorption isotherm

Adsorption characteristics of PFOA onto the X/XO_y-CNTs and MWCNTs were exhibited in Fig. 3. Based on the characteristics of adsorption on MWCNTs [50,51], Henry model and Freundlich model were leveraged suitably for fitting the adsorption isotherms data and the regression parameters were illustrated in Table S3. Compared with Henry model, Freundlich model was better to reflect the isotherms due to its relative higher r_{adj}^2 . Thus, the discussion followed was in view of the adsorption parameters obtained by calculating from the Freundlich

model fitting results.

Cu/CuO-CNTs had the best adsorption among the four adsorbents, and the adsorption amounts on Fe/Fe₂O₃-CNTs and Zn/ZnO-CNTs were also higher than on MWCNTs (Fig. 3A). For eliminating the effect of SSA, the adsorption data were normalized by surface area and presented in Fig. 3B, the adsorption tendency was not significantly altered, which demonstrated that the surface area was not the only crucially contributing factor in the adsorption process.

The adsorption amount of PFOA decreased with the increasing numbers of hydroxyl, carboxyl and/or carbonyl groups on the surface of MWCNTs, which was attributed to the weakness of the hydrophobic interaction between MWCNTs and PFOA [35]. However, X/XO_y-CNTs

owned the opposite results (Table S3). In low PFOA concentration (e.g. $C_e = 20 \mu\text{g L}^{-1}$), the Cu/CuO-CNTs had the biggest adsorption capacity which was about 17.99-fold of MWCNTs, and the Fe/Fe₂O₃-CNTs own almost 2.98 times of the primitive one. The adsorption capacity of Zn/ZnO-CNTs illustrated 1.98 times higher than that of MWCNTs.

3.2.3. Desorption isotherm

The adsorption-desorption isotherms of PFOA on each adsorbents were shown in Fig. S6. After six desorption processes, the desorption rate of PFOA on Fe/Fe₂O₃-CNTs, Cu/CuO-CNTs, Zn/ZnO-CNTs and MWCNTs were 13.29%, 3.36%, 16.47% and 52.56% of their maximum adsorption amount, respectively. It can be clearly seen from the results of desorption experiments that the Cu/CuO-CNTs were the most strongly linked with PFOA, and only a small fraction of PFOA molecules (3%–4%) were separated from the adsorbent after the repeated desorption. By the comparison, more than half adsorbed PFOA molecules on MWCNTs were shed after six times of desorption. The binding of Fe/Fe₂O₃-CNTs and Zn/ZnO-CNTs with PFOA molecules were also relatively tight than MWCNTs. It was the inner-sphere complexes formed between PFOA molecules and MNPs, which was much stronger than the hydrophobic interaction or electrostatic interaction.

3.2.4. Adsorption mechanism

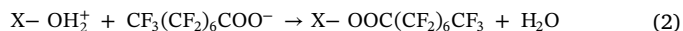
The adsorption of PFOA by X/XO_y-CNTs involved a variety of interactions, and these interactions were visually expressed in Fig. 4. In the process of acidic treatment and modification of MNPs, some oxygen functional groups inevitably induced on the surface of MWCNTs and even formed X–OH (X=Fe, Cu and Zn) constitution [56]. It was important to point out that a large amount of –OH exists on the MNPs surface. Besides, PFOA is one kind of monocarboxylic acid, and the pK_a value was lower than the pH adopted in this study. Therefore, PFOA completely existed in the form of deprotonated PFOA[–] (CF₃(CF₂)₆COO[–]).

The metal processed two kinds of combination with MWCNTs. The first one was metal element and C atom connected by O atom to form metal–O–C bond. The other one was to form a metal–C bond. The XPS analysis provided useful information about chemical composition. The binding energies gotten in XPS analysis were calibrated for the specimen charging by referencing the C 1s peak to 284.6 eV. Fig. 5, S4 and S5 illustrated the XPS spectras of C 1s, O 1s and X 2p peaks of X/XO_y-CNTs and MWCNTs after adsorbing PFOA, respectively.

The XPS spectra of C 1s shown in Fig. 5 were asymmetric, indicating that multi-component carbon species were present on the surface. Amorphous carbon and/or graphite carbon (C–C/C=C) were the dominant speciation of C in the X/XO_y-CNTs and MWCNTs at 284.7 eV [52,53]. Compared with the MWCNTs, the doped ones increased the percentage of peaks at 285.5 ± 0.4 eV and 288.6 ± 0.5 eV, indicating that the increased of C–O and C=O bonds on the X/XO_y-CNTs [52,53]. Binding energies at 291.6 ± 0.2 eV and 294.2 ± 0.4 eV were characteristic peaks of –CF₂ and –CF₃ of PFOA [54]. Besides, a new peak appeared at 283.5 eV (Fig. 5A), which contributed to the formation of Fe–C bond [55]. The same weak peaks were attributed to Cu–C (283.8 eV, Fig. 5B), Zn–C bond (284.3 eV, Fig. 5C). This confirmed metal–C bonds formed directly between metal and MWCNTs.

For X/XO_y-CNTs, hydrolysis reaction of –OH on the surface of MNP led to a large number of positive charges on the surface of MNPs (Eq. (1)), and PFOA[–] were adsorbed to the MNPs surface by electrostatic interaction, and complex reactions were formed to shape the inner-sphere complexes. This brought about the inner-sphere complexes formation by ligand exchange between carboxylate head groups of PFOA and X–OH constitution on the adsorbents (Eq. (2)) [56]. Thus a part of PFOA was adsorbed on the surface of MWCNTs by covalent bond with X atom. After that, the hydrophobic tail of PFOA can form hydrophobic interaction with the free PFOA molecule in the solution, and further increase the adsorption amount of PFOA. It must be pointed out that a part of water molecules were catalytic decomposed into H and

OH by CuO, and then the *p* orbital of the O atoms coming from OH combined with the *d* orbital of the Cu atoms, making the OH tightly bind to the CuO surface [57]. In contrast, Fe₂O₃ and ZnO did not have this catalytic process. This provided more opportunities for PFOA to adsorb with CuO than Fe₂O₃ and ZnO. It also explained the phenomenon that the content of Cu was the lowest in three complex substances (Table 1) and the adsorption capacity of CuO-CNTs was the highest (Fig. 3A). Since a part of ZnO were dissolved at pH 6.50 [58], the amount of Fe/Fe₂O₃-CNTs and Cu/CuO-CNTs adsorbed on PFOA were higher than that of Zn/ZnO-CNTs. In addition, on the MWCNTs surface where no MNPs were loaded, the PFOA were mainly adsorbed by the hydrophobic interaction [35].



Moreover, besides the electrostatic interaction was involved when the PFOA were adsorbed on MNPs, relatively weak ion-dipole interaction could be formed between anionic PFOA molecules and polar functionalities (such as –OH) [60]. Compared with the hydrophobic force and electrostatic force, normal hydrogen bonds played a relatively small role in the adsorption of PFOA. Because the zero potential point of MWCNTs were lower than the experimental condition (pH 6.50, Fig. S2), the functional groups of MWCNTs were deprotonated, and thus it was difficult to form normal hydrogen bonds. However, in this case charge-assisted hydrogen bonds ((–)CAHB) could form and enhanced the adsorption of PFOA [59].

3.3. Effects of environmental factors

3.3.1. Effects of ionic strength

The initial concentration of PFOA was selected $200 \mu\text{g L}^{-1}$ to study the influence of ionic strength in the range of 0–100 mM (Fig. 6). In general, ionic strength had a little effect on the adsorbed amounts of PFOA on the X/XO_y-CNTs, and especially on Cu/CuO-CNTs had almost no influence. In contrast, the adsorption amount of PFOA increased 3.67 fold with increasing NaCl concentration from 0 to 100 mM for MWCNTs.

The ionic strength mainly affected the PFOA adsorption through two aspects. On the one hand, the ionic strength can inhibit adsorption by forming pyknotic structures through adsorbents aggregation [61]. On the other hand, the increase of ionic strength also promotes adsorbing the organic matter because of the electrostatic shielding effect or salting-out effect [62]. If the former one is the dominant factor, the adsorbed amount of PFOA be thus decreased with ionic strength increasing. On the contrary, the adsorption of PFOA increased if the latter effect of is stronger than that of the former as increasing ionic strength. Especially under high ionic strength conditions, the salting-out effect plays an important role because salt can promote the transfer of PFOA molecules from salt solution to adsorbents (Part III 4 of Supplementary data) [47].

3.3.2. Effect of ionic species

The effects of ionic species on PFOA adsorption were illustrated in Fig. S7. Ca²⁺ substituting Na⁺ slightly increased the adsorption amount of PFOA, especially for MWCNTs. The surface of the adsorbents were negatively charged, since the pH value in the medium was higher than pH_{zpc} , and Ca²⁺ had competence to form a cation bridge between the deprotonated PFOA molecules and adsorbents, especially surface hydroxyl or carboxyl groups, to increase the adsorption amount of PFOA (Fig. S7D) [63]. Of course, Ca²⁺ also formed a bridge between two PFOA molecules, which induced the formation of PFOA complexes, so that it could also increase the adsorption amount of PFOA by hydrophobic interaction to a certain extent.

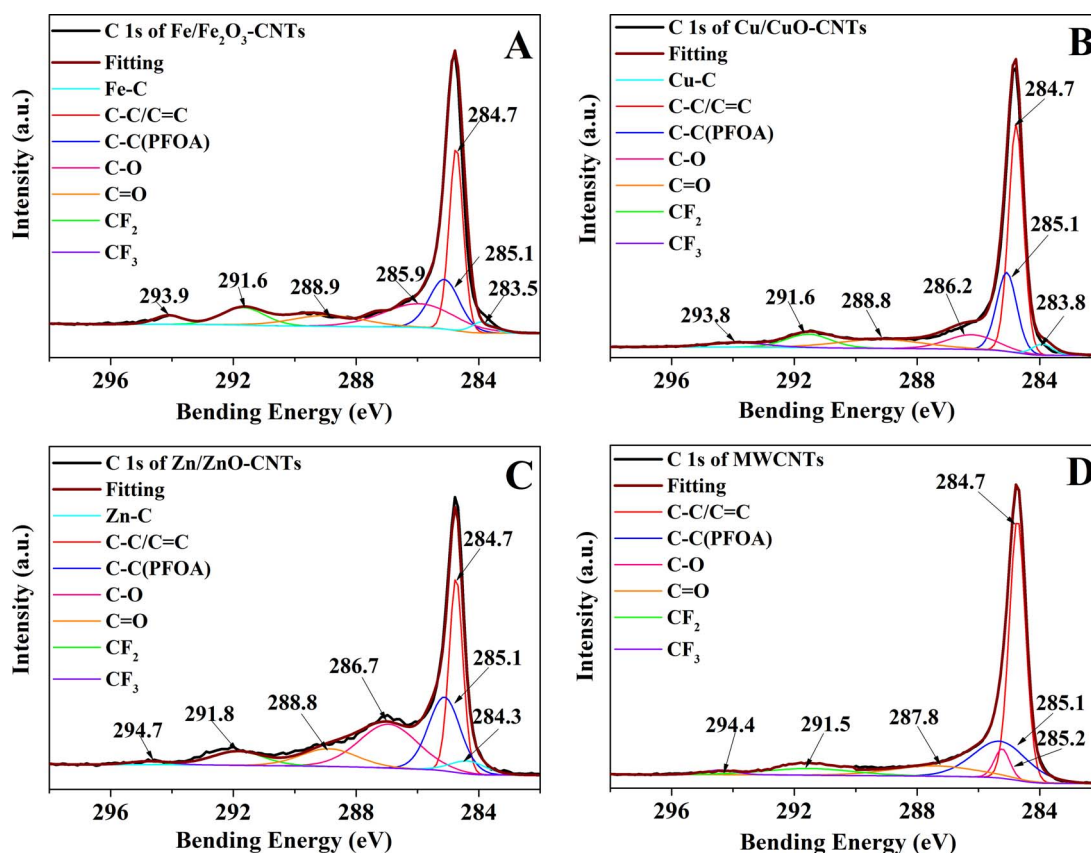


Fig. 5. C 1s XPS spectrum of (A) Fe/Fe₂O₃-CNTs, (B) Cu/CuO-CNTs, (C) Zn/ZnO-CNTs and (D) MWCNTs after PFOA adsorption.

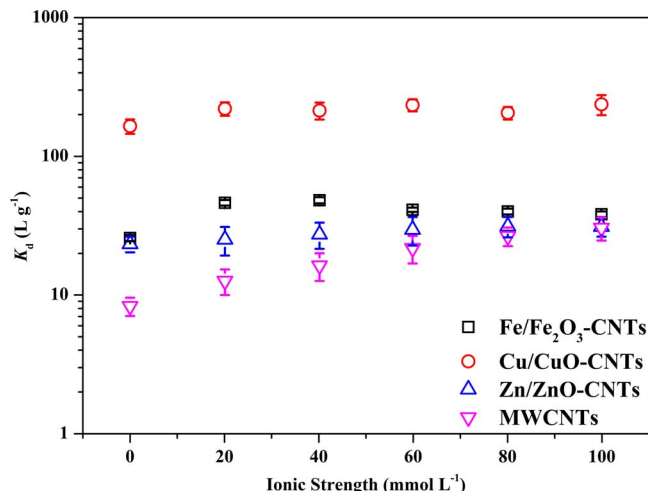


Fig. 6. Effect of Ionic strength (NaCl, 0–100 mM) on distribution coefficient (K_d) for single point adsorption of PFOA onto X/XO_y-CNTs and MWCNTs. Initial concentration of PFOA was 200 μ g L⁻¹ and the pH of electrolyte solution was 6.50 ± 0.10 .

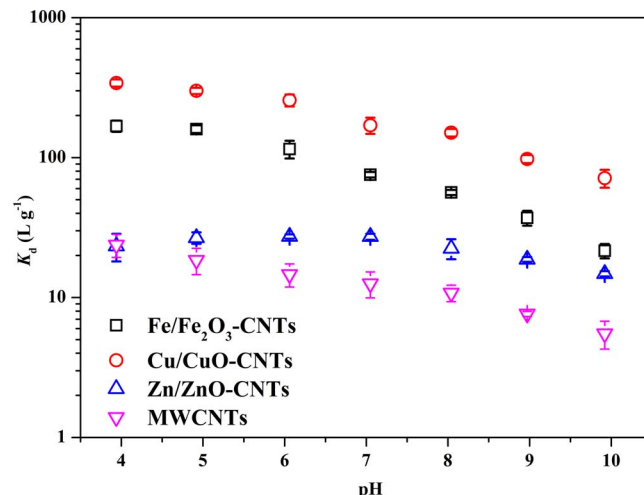


Fig. 7. Effect of pH on distribution coefficient (K_d) for single point adsorption of PFOA onto X/XO_y-CNTs and MWCNTs in 10 mM NaCl.

3.3.3. Effects of pH

The effects of pH on the adsorption of PFOA by adsorbents are displayed in Fig. 7. The association of functional groups on the adsorbents was obviously affected by pH value in the electrolyte solution. For MWCNTs, its adsorption showed a strong dependence on pH value, i.e., the adsorption of PFOA increased under acidic conditions, and alkaline condition apparently inhibited the PFOA adsorption. As the pH increased from 3.94 to 9.92, adsorption of Fe/Fe₂O₃-CNTs, Cu/CuO-CNTs and MWCNTs decreased 87.16%, 79.08% and 76.81%, respectively. Because of the special amphoteric properties of ZnO, the adsorbed amount of Zn/ZnO-CNTs was decreased 45.84% from pH 7.05 to

9.92.

In the condition of low pH, the ionic strength of the electrolyte solution would increase due to the dissolution of metal ions [58,64], and at the same time, the dissolved ions formed bridge between PFOA molecules and X/XO_y-CNTs, which resulted in an increasing adsorption amount. In addition, it was also one of reasons to increase the adsorption amount that the number of protonation adsorption sites would be increased under acidic conditions [65]. Firm covalent bond was formed between the X/XO_y-CNTs and PFOA molecules. So that the complexes occupied the most adsorption sites on the X/XO_y-CNTs surface, while electrostatic attraction did not increase lots of adsorption amount at pH 3.94. In OH⁻ abundant electrolyte solution, the

adsorption of PFOA was much reduced on each adsorbent. Because increasing pH value would increase the competition between OH^- and PFOA^- , and reduce the hydrophobic interaction between PFOA molecules and adsorbents [66]. Furthermore, electrostatic repulsion enhanced with the increase of pH value, and it would also inhibit the adsorption between PFOA molecules and adsorbents [67].

In general, X/XO_y-CNTs showed excellent adsorption effects under low PFOA equilibrium concentrations ($1.07 \mu\text{g L}^{-1}$ – $1.54 \cdot 10^2 \mu\text{g L}^{-1}$) in aqueous medium. Most importantly, the concentration of PFOA is generally ng L^{-1} to $\mu\text{g L}^{-1}$ level in the natural environment water [11]. However, the study of the adsorption behavior of PFOA at such a low equilibrium concentration rarely has been reported. Although it was reported that the adsorption amount of PFOA on activated carbon was higher than that of MWCNTs [35], but that was under the condition of high PFOA concentration ($> 40,000 \mu\text{g L}^{-1}$), and it had little practical significance in removing PFOA from environmental media. Under low PFOA concentration (e.g. $20 \mu\text{g L}^{-1}$), the adsorption amount of activated carbon was not high ($74.43 \mu\text{g g}^{-1}$) [25], even lower than MWCNTs ($2.75 \cdot 10^2 \mu\text{g g}^{-1}$).

4. Conclusions

Nano-metals and its oxides doped MWCNTs were characterized by TEM, XRD, FTIR and XPS. Adsorption kinetics showed the mainly governed step of PFOA adsorption on X/XO_y-CNTs was intra-particle diffusion. PFOA adsorption affinity on the X/XO_y-CNTs, especially on Cu/CuO-CNTs, were higher than MWCNTs. PFOA adsorption-desorption on X/XO_y-CNTs were not reversible processes. PFOA adsorbed on X/XO_y-CNTs mainly resulted from the formation of inner-sphere complexes, hydrophobic interaction and electrostatic interaction. At low ionic strength (0–20 mM), the adsorption amounts of PFOA on X/XO_y-CNTs slightly increased, and at ionic strength range (20–100 mM), the adsorption amounts were basically unchanged. The promotion effect of Ca^{2+} on X/XO_y-CNTs was not pronounced in comparison with the presence of Na^+ . The pH value of electrolyte solution had great influence on the adsorption of PFOA. The acidic condition promoted the adsorption, and the alkaline condition obviously inhibited the adsorption. According to the results of this study, X/XO_y-CNTs had good adsorption efficiency on trace PFOA in water environment, which will be of great help for practical applications in the future.

Acknowledgments

This work was financially supported by the National Nature Science Foundation of China (Project No. 21377074) and Collaborative Fund between National Nature Science Foundation of China and Swiss National Science Foundation (Project No. 21661132004).

Appendix A. Supplementary data

Supplementary material related to this article can be found, in the online version, at doi:<https://doi.org/10.1016/j.jhazmat.2018.03.001>.

References

- [1] Z. Liu, Y. Lu, T. Wang, P. Wang, Q. Li, A.C. Johnson, S. Sarvajayakesavalu, A.J. Sweetman, Risk assessment and source identification of perfluoroalkyl acids in surface and ground water: Spatial distribution around a mega-fluorochemical industrial park, China, *Environ. Int.* 91 (2016) 69–77.
- [2] T. Wang, W. Pei, M. Jing, S. Liu, Y. Lu, J.S. Khim, J.P. Giesy, A review of sources, multimedia distribution and health risks of perfluoroalkyl acids (PFAAs) in China, *Chemosphere* 129 (2014) 87–99.
- [3] A.B. Lindstrom, M.J. Strynar, E.L. Libelo, Polyfluorinated compounds: Past, present, and future, *Environ. Sci. Technol.* 45 (2011) 7954–7961.
- [4] K. Prevedouros, I.T. Cousins, R.C. Buck, S.H. Korzeniowski, Sources, fate and transport of perfluorocarboxylates, *Environ. Sci. Technol.* 40 (2006) 32–44.
- [5] S. Posner, Perfluorinated compounds: Occurrence and uses in products, in: T.P. Knepper, F.T. Lange (Eds.), *Polyfluorinated Chemicals and Transformation Products*, Springer, Heidelberg, 2012, pp. 25–39.
- [6] OECD. OECD/UNEP Global PFC Group, Synthesis Paper on Per- and Polyfluorinated Chemicals (PFCs), Environment Directorate, Organisation for Economic Co-operation and Development (OECD), Paris, 2013.
- [7] S.T. Washburn, T.S. Bingman, S.K. Braithwaite, R.C. Buck, L.W. Buxton, H.J. Clewell, L.A. Haroun, J.E. Kester, R.W. Rickard, A.M. Shipp, Exposure assessment and risk characterization for perfluorooctanoate in selected consumer articles, *Environ. Sci. Technol.* 39 (2005) 3904–3910.
- [8] M. Hudlicky, Hydrogenolysis of carbon-fluorine bonds in catalytic hydrogenation, *J. Fluor. Chem.* 14 (1979) 189–199.
- [9] H. Yoo, J.W. Washington, J.J. Ellington, T.M. Jenkins, M.P. Neill, Concentrations, distribution, and persistence of fluorotelomer alcohols in sludge-applied soils near Decatur, Alabama, USA, *Environ. Sci. Technol.* 44 (2010) 8397–8402.
- [10] J. Li, S.D. Vento, J. Schuster, G. Zhang, P. Chakraborty, Y. Kobara, D.C. Jones, Perfluorinated compounds in the Asian atmosphere, *Environ. Sci. Technol.* 45 (2011) 7241–7248.
- [11] X. Feng, F.S. Matt, R.H. Thomas, S.G. John, Perfluorooctane sulfonate (PFOS) and perfluorooctanoate (PFOA) in soils and groundwater of a U.S. metropolitan area: Migration and implications for human exposure, *Water Res.* 72 (2015) 64–74.
- [12] C.E. Müller, A.O. Silva, J. Small, M. Williamson, X. Wang, A. Morris, S. Katz, Biomagnification of perfluorinated compounds in a remote terrestrial food chain: Lichen–Caribou–Wolf, *Environ. Sci. Technol.* 45 (2011) 8665–8673.
- [13] W. D'Hollander, P. Voogt, W. Coen, L. Bervoets, Perfluorinated substances in human food and other sources of human exposure, *Rev. Environ. Contam. Toxicol.* 208 (2010) 179–215.
- [14] E. Mariussen, Neurotoxic effects of perfluoroalkylated compounds: Mechanisms of action and environmental relevance, *Arch. Toxicol.* 86 (2012) 1349–1367.
- [15] C. Lau, J.L. Butenhoff, J.M. Rogers, The developmental toxicity of perfluoroalkyl acids and their derivatives, *Toxicol. Appl. Pharmacol.* 198 (2004) 231–241.
- [16] K.S. Betts, Perfluoroalkyl acids: What is the evidence telling us? *Environ. Health Perspect.* 115 (2007) A344.
- [17] K. Li, C. Li, N.Y. Yu, A.L. Juhasz, X.Y. Cui, L.Q. Ma, In vivo bioavailability and in vitro bioaccessibility of perfluorooctanoic acid (PFOA) in food matrices: Correlation analysis and method development, *Environ. Sci. Technol.* 49 (2015) 150–158.
- [18] J.W. Washington, T.M. Jenkins, Abiotic hydrolysis of fluorotelomer-based polymers as a source of perfluorocarboxylates at the global scale, *Environ. Sci. Technol.* 49 (2015) 14129–14135.
- [19] H. Hori, Y. Nagaoka, M. Murayama, S. Kutsuna, Efficient decomposition of perfluorocarboxylic acids and alternative fluorocarbon surfactants in hot water, *Environ. Sci. Technol.* 42 (2008) 7438–7443.
- [20] C.D. Vecitis, Y. Wang, J. Cheng, H. Park, B.T. Mader, M.R. Hoffmann, Sonochemical degradation of perfluorooctane sulfonate in aqueous film-forming foams, *Environ. Sci. Technol.* 44 (2010) 432–438.
- [21] X. Li, P. Zhang, L. Jin, T. Shao, Z. Li, J. Cao, Efficient photocatalytic decomposition of perfluorooctanoic acid by indium oxide and its mechanism, *Environ. Sci. Technol.* 46 (2012) 5528–5534.
- [22] S. Horikoshi, S. Sato, M. Abe, N. Serpone, A novel liquid plasma AOP device integrating microwaves and ultrasounds and its evaluation in defluorinating perfluorooctanoic acid in aqueous media, *Ultrason. Sonochem.* 18 (2011) 938–942.
- [23] H.W. Sun, F.S. Li, T. Zhang, X.Z. Zhang, N. He, Q. Song, L.J. Zhao, L.N. Sun, T.H. Sun, Perfluorinated compounds in surface waters and WWTPs in Shenyang, China: Mass flows and source analysis, *Water Res.* 45 (2011) 4483–4490.
- [24] C.L. Li, A. Schäffer, J.M. Séquaris, K. László, A. Tóth, E. Tombácz, H. Vereecken, R. Ji, E. Klumpp, Surface-associated metal catalyst enhances the sorption of perfluorooctanoic acid to multi-walled carbon nanotubes, *J. Colloid Interface Sci.* 377 (2012) 342–346.
- [25] D. Zhang, Q. Luo, B. Gao, S.-Y.D. Chiang, D. Woodward, Sorption of perfluorooctanoic acid, perfluorooctane sulfonate and perfluoroheptanoic acid on granular activated carbon, *Chemosphere* 144 (2016) 2336–2342.
- [26] Q. Yu, S.B. Deng, G. Yu, Selective removal of perfluorooctane sulfonate from aqueous solution using chitosan-based molecularly imprinted polymer adsorbents, *Water Res.* 42 (2008) 3089–3097.
- [27] Q.Y. Zhang, S.B. Deng, G. Yu, J. Huang, Removal of perfluorooctane sulfonate from aqueous solution by crosslinked chitosan beads: Sorption kinetics and uptake mechanism, *Bioresour. Technol.* 102 (2011) 2265–2271.
- [28] Q. Zhou, S.B. Deng, Q.Y. Zhang, Q. Fan, J. Huang, G. Yu, Sorption of perfluorooctane sulfonate and perfluorooctanoate on activated sludge, *Chemosphere* 81 (2010) 453–458.
- [29] C.P. Higgins, R.G. Luthy, Sorption of perfluorinated surfactants on sediments, *Environ. Sci. Technol.* 40 (2006) 7251–7256.
- [30] Y. Wang, J. Niu, Y. Li, T. Zheng, Y. Xu, Y. Liu, Performance and mechanisms for removal of perfluorooctanoate (PFOA) from aqueous solution by activated carbon fiber, *RSC Adv.* 5 (2015) 86927–86933.
- [31] J. Thompson, G. Eaglesham, J. Reungoat, Y. Poussade, M. Bartkow, M. Lawrence, J.F. Mueller, Removal of PFOS, PFOA and other perfluoroalkyl acids at water reclamation plants in south east Queensland Australia, *Chemosphere* 82 (2011) 9–17.
- [32] Y.P. Bao, J.F. Niu, Z.S. Xu, D. Gao, J.H. Shi, X.M. Sun, Q.G. Huang, Removal of perfluorooctane sulfonate (PFOS) and perfluorooctanoate (PFOA) from water by coagulation: Mechanisms and influencing factors, *J. Colloid Interface Sci.* 434 (2014) 59–64.
- [33] B. Pan, B.S. Xing, Adsorption mechanisms of organic chemicals on carbon nanotubes, *Environ. Sci. Technol.* 42 (2008) 9005–9013.
- [34] X. Chen, X.H. Xia, X.L. Wang, J.P. Qiao, H. Chen, A comparative study on sorption of perfluorooctane sulfonate (PFOS) by chars, ash and carbon nanotubes, *Chemosphere* 83 (2011) 1313–1319.
- [35] S.B. Deng, Q.Y. Zhang, Y. Nie, H.R. Wei, B. Wang, J. Huang, G. Yu, B.S. Xing, Sorption mechanisms of perfluorinated compounds on carbon nanotubes, *Environ.*

- Pollut. 168 (2012) 138–144.
- [36] Y.F. Sun, C.S. Li, A. Zhang, Preparation of Ni/CNTs catalyst with high reducibility and their superior catalytic performance in benzene hydrogenation, *Appl. Catal., A: Gen.* 522 (2016) 180–187.
- [37] D. Ganguly, D. Pahari, N.S. Das, P. Howli, B. Das, D.K.K. Banerjee, Chattopadhyay, all-amorphous CNT-MnO₂ nanoflake hybrid for improved super capacitor applications, *J. Electroanal. Chem.* 778 (2016) 12–22.
- [38] C.L. Dai, M.Q. Wang, J.G. Yang, L.Y. Hu, M.W. Xu, Fabrication of MnO@C-CNTs composite by CVD for enhanced performance of lithium ion batteries, *Ceram. Int.* 42 (2016) 18568–18572.
- [39] S.S. Wang, B. Gao, Y.C. Li, A.E. Creamer, F. He, Adsorptive removal of arsenate from aqueous solutions by biochar supported zero-valent iron nanocomposite: Batch and continuous flow tests, *J. Hazard. Mater.* 322 (2016) 172–181.
- [40] X.Y. Wang, F. Zhang, B.Y. Xia, X.F. Zhu, J.S. Chen, S.L. Qiu, P. Zhang, J.X. Li, Controlled modification of multi-walled carbon nanotubes with CuO, Cu₂O and Cu nanoparticles, *Solid State Sci.* 11 (2009) 655–659.
- [41] M. Engel, B. Chefetz, Adsorption and desorption of dissolved organic matter by carbon nanotubes: Effects of chemistry, *Environ. Pollut.* 213 (2016) 90–98.
- [42] H.P. Boehm, Surface oxides on carbon and their analysis: A critical assessment, *Carbon* 40 (2002) 145–149.
- [43] A. Chakravarty, D. Sengupta, B. Basu, A. Mukherjee, G. De, MnO₂ nanowires anchored on amine functionalized graphite nanosheets: Highly active and reusable catalyst for organic oxidation reactions, *RSC Adv.* 5 (2015) 92585–92595.
- [44] J.S. Zhou, H.H. Song, L.L. Maab, X.H. Chen, Magnetite/Graphene nanosheet composites: Interfacial interaction and its impact on the durable high-rate performance in lithium-ion batteries, *RSC Adv.* 1 (2011) 782–791.
- [45] Y.C. Si, E.T. Samulski, Exfoliated graphene separated by platinum nanoparticles, *Chem. Mater.* 20 (2008) 6792–6797.
- [46] N.W.C. Jusoh, A.A. Jalil, S. Triwahyono, H.D. Setiabudi, N. Sapawe, M.A.H. Satar, A.H. Karim, N.H.N. Kamarudin, R. Jusoh, N.F. Jaafar, N. Salamun, J. Efendi, Sequential desilication–isomorphous substitution route to prepare mesostructured silica nanoparticles loaded with ZnO and their photocatalytic activity, *Appl. Catal., A* 468 (2013) 276–287.
- [47] F. Liu, J. Zhao, S. Wang, P. Du, B. Xing, Effects of solution chemistry on adsorption of selected pharmaceuticals and personal care products (PPCPs) by graphenes and carbon nanotubes, *Environ. Sci. Technol.* 48 (2014) 13197–13206.
- [48] O.G. Apul, T. Shao, S. Zhang, T. Karanfil, Impact of carbon nanotube morphology on phenanthrene adsorption, *Environ. Toxicol. Chem.* 31 (2012) 73–78.
- [49] Y. Qu, C.J. Zhang, F. Li, X.W. Bo, G.F. Liu, Q. Zhou, Equilibrium and kinetics study on the adsorption of perfluorooctanoic acid from aqueous solution onto powdered activated carbon, *J. Hazard. Mater.* 169 (2009) 146–152.
- [50] Y. Bei, S.B. Deng, Z.W. Du, B. Wang, J. Huang, G. Yu, Adsorption of perfluorooctane sulfonate on carbon nanotubes: Influence of pH and competitive ions, *Water Sci. Technol.* 69 (2014) 1489–1495.
- [51] C.M. Xu, H. Chen, F. Jiang, Adsorption of perfluorooctane sulfonate (PFOS) and perfluorooctanoate (PFOA) on polyaniline nanotubes, *Colloids Surf. A* 479 (2015) 60–67.
- [52] A. Bagri, C. Mattevi, M. Acik, Y.J. Chabal, M. Chhowalla, V.B. Shenoy, Structural evolution during the reduction of chemically derived graphene oxide, *Nat. Chem.* 2 (2010) 581–587.
- [53] X. Hu, Z.H. Ding, A.R. Zimmerman, S.S. Wang, B. Gao, Batch and column sorption of arsenic onto iron-impregnated biochar synthesized through hydrolysis, *Water Res.* 68 (2015) 206–216.
- [54] C.W. Zhao, J. Fan, D. Chen, Y. Xu, T. Wang, Microfluidics-generated graphene oxide microspheres and their application to removal of perfluorooctane sulfonate from polluted water, *Nano Res.* 9 (2016) 866–875.
- [55] A. Adenier, M.C. Bernard, M.M. Chehimi, E. Cabet-Deliry, B. Desbat, O. Fagebaume, J. Pinson, F. Podvorica, Covalent modification of iron surfaces by electrochemical reduction of aryldiazonium salts, *J. Am. Chem. Soc.* 123 (2001) 4541–4549.
- [56] X.D. Gao, J. Chorover, Adsorption of perfluorooctanoic acid and perfluorooctane sulfonic acid to iron oxide surfaces as studied by flow-through ATR-FTIR spectroscopy, *Environ. Chem.* 9 (2012) 148–157.
- [57] J. Zhang, R.G. Zhang, B.J. Wang, L.X. Ling, Insight into the adsorption and dissociation of water over different CuO(111) surfaces: The effect of surface structures, *Appl. Surf. Sci.* 364 (2016) 758–768.
- [58] F.M. Omar, H.A. Aziz, S. Stoll, Aggregation and disaggregation of ZnO nanoparticles: Influence of pH and adsorption of Suwannee River humic acid, *Sci. Total Environ.* 468–469 (2014) 195–201.
- [59] X. Li, J.J. Pignatello, Y. Wang, B. Xing, New insight into adsorption mechanism of ionizable compounds on carbon nanotubes, *Environ. Sci. Technol.* 47 (2013) 8334–8341.
- [60] A.H. Karoyo, L.D. Wilson, Tunable macromolecular-based materials for the adsorption of perfluorooctanoic and octanoic acid anions, *J. Colloid Interface Sci.* 402 (2013) 196–203.
- [61] H.H. Cho, H. Huang, K. Schwab, Effects of solution chemistry on the adsorption of ibuprofen and triclosan onto carbon nanotubes, *Langmuir* 27 (2011) 12960–12967.
- [62] S. Zhang, T. Shao, S.S.K. Bekaroglu, T. Karanfil, Adsorption of synthetic organic chemicals by carbon nanotubes: Effects of background solution chemistry, *Water Res.* 44 (2010) 2067–2074.
- [63] Y.N. Kwon, K. Shih, C. Tang, J.O. Leckie, Adsorption of perfluorinated compounds on thin-film composite polyamide membranes, *J. Appl. Polym. Sci.* 124 (2012) 1042–1049.
- [64] A.J. Bard, L.R. Faulkner, *Electrochemical Methods Fundamentals and Applications*, 2nd ed., John Wiley and Sons, Inc., 2001, pp. 140–146 Chapter 4.
- [65] B.K. Pramanika, S.K. Pramanik, F. Suja, A comparative study of coagulation, granular- and powdered-activated carbon for the removal of perfluorooctane sulfonate and perfluorooctanoate in drinking water treatment, *Environ. Technol.* 36 (2015) 2610–2617.
- [66] L. Ji, W. Chen, S. Zheng, Z. Xu, D. Zhu, Adsorption of sulfonamide antibiotics to multiwalled carbon nanotubes, *Langmuir* 25 (2009) 11608–11613.
- [67] Z. Wang, X. Yu, B. Pan, B. Xing, Norfloxacin sorption and its thermodynamics on surface-modified carbon nanotubes, *Environ. Sci. Technol.* 44 (2009) 978–984.